

PROBLEMES D'ONDES
WAVES PROBLEMS

THREE DIMENSIONAL FLOWS AROUND AIRFOILS WITH SHOCKS

Antony Jameson

Courant Institute of Mathematical Sciences, New York University

1. Introduction.

The determination of flows containing embedded shock waves over a wing in a stream moving at near sonic speed is an important engineering problem. The economy of operation of a transport aircraft is generally improved by increasing its speed to the point at which the drag penalty due to the appearance of shock waves begins to overbalance the savings obtainable by flying faster. Thus the transonic regime is precisely the regime of greatest interest in the design of commercial aircraft. The calculation of transonic flows also poses a problem which is mathematically interesting, because the governing partial differential equation is nonlinear and of mixed type, and it is necessary to admit discontinuities in order to obtain a solution.

The recent development of successful numerical methods for calculating two dimensional transonic flows around airfoils (Murman and Cole, 1971, Steger and Lomax 1972; Garabedian and Korn 1972; Jameson 1971) encourages the belief that it should be possible to perform useful calculations of three dimensional flows with the existing generation of computers such as the CDC 6600 and 7600. The flow over an isolated yawed wing appears to be particularly suitable for a first attack. While the boundary shape is relatively simple, this configuration includes the full complexities of a three dimensional flow with oblique shock waves and a trailing vortex sheet. At the same time the use of a yawed wing has been seriously proposed for a transonic transport (Jones, 1972) because it can generate lift with less wave drag than an arrow wing, and detailed design studies and tests are presently being conducted.

In setting up a mathematical model we are guided by the need to obtain equations which are simple enough for their solution to be feasible, while at the same time retaining the important characteristics of the real flow. In the case of flows around airfoils viscous effects take place in a much smaller length scale than the main flow. Accordingly they will be ignored except for their role in preventing flow around the sharp trailing edge, thus inducing circulation and lift. With this simplification the mathematical difficulties are principally caused by the mixed elliptic and hyperbolic type of the equations, and by the presence of shock waves. A satisfactory method should be capable of predicting the onset of wave drag if not its

exact magnitude. Since strong shock waves would lead to high drag, we may reasonably suppose that an efficient aerodynamic design would permit only the presence of quite weak shock waves, so that the error in ignoring variations in entropy and assuming an irrotational flow should be small. The proper treatment of strong shock waves would require a much more complicated model, allowing for the presence of regions of separated flow behind the shock waves. Thus we are led to use the potential equation for irrotational flow:

$$(a^2 - u^2)\phi_{xx} + (a^2 - v^2)\phi_{yy} + (a^2 - w^2)\phi_{zz} - 2uv\phi_{xy} - 2vw\phi_{yz} - 2vw\phi_{xy} = 0 \quad (1)$$

in which ϕ is the velocity potential, u , v and w are the velocity components

$$u = \phi_x, \quad v = \phi_y, \quad w = \phi_z \quad (2)$$

and a is the local speed of sound. This is determined from the stagnation speed of sound a_0 by the energy relation

$$a^2 = a_0^2 - \frac{\gamma-1}{2} (u^2 + v^2 + w^2) \quad (3)$$

where γ is the ratio of the specific heats. This equation is elliptic at subsonic points where

$$a^2 > u^2 + v^2 + w^2$$

and hyperbolic at supersonic points where

$$a^2 < u^2 + v^2 + w^2$$

It is to be solved subject to the Neumann boundary condition

$$\frac{\partial \phi}{\partial n} = 0 \quad (4)$$

at the wing surface, where n is the normal direction. Since smooth transonic solutions are known not to exist except for special boundary shapes (Morawetz, 1956), it is necessary to admit weak solutions (Lax, 1954). The appropriate jump conditions require conservation of the normal component of mass flow and the tangential component of velocity. Since the potential equation represents isentropic flow, the normal component of momentum is then not conserved, so that the jump carries a force which is balanced by an opposing force on the body. Thus a drag force appears, providing an approximate representation of wave drag. The method can therefore be used to predict drag rise due to the appearance of shock waves.

The use of one dependent variable instead of the five required by

the full Euler equations (u, v, w , density and energy) is an important advantage for three dimensional calculations, which are generally restricted by limitations of machine memory. A further simplification can be obtained by using small disturbance theory, in which only the first term of an expansion in a thickness parameter is retained (Bailey and Ballhouse, 1972). Equation (1) is replaced by

$$(1-M_\infty^2 - (\gamma+1)M_\infty^2 \phi_x^2) \phi_{xx} + \phi_{yy} + \phi_{zz} = 0 \quad (5)$$

where M_∞ is the Mach number at infinity. The boundary condition is now applied at the plane $z = 0$, eliminating the need to satisfy a Neumann boundary condition at a curved surface. Such an expansion is not uniformly valid, however, failing near stagnation points on blunt leading edges. Since it is desired to resolve the effects of small changes in the shape of the wing section, which may be required to limit the strength of shock waves appearing in the flow, or even to obtain shock-free flow (Bauer, Garabedian and Korn, 1972), it is preferred here to use the full potential flow equation (1).

Solutions of the potential equation are invariant under a reversal of flow direction

$$u = -\phi_x, \quad v = -\phi_y, \quad w = -\phi_z$$

and in the absence of a directional condition corresponding to the condition that entropy can only increase, its solution in the transonic regime is not unique. Solutions with expansion shocks are possible. To exclude these, and to ensure uniqueness, the directional property which was removed by eliminating entropy from the equations must be restored in the numerical scheme. This indicates the need to use biased differencing in the supersonic zone, corresponding to the upwind region of dependence of the flow. For the small disturbance equation (5) this can be achieved simply by using backward difference formulas in the x direction at all supersonic points (Murman and Cole 197). At the point $i\Delta x, j\Delta y, k\Delta y$, ϕ_{xx} is represented by

$$\frac{\phi_{i,j,k} - 2\phi_{i-1,j,k} + \phi_{i-2,j,k}}{\Delta x^2}$$

The dominant truncation error $-\Delta x \phi_{xxx}$ arising from this expression then acts as an artificial viscosity, since the coefficient of ϕ_{xx} is negative in the supersonic zone. This ensures that only the proper jumps can occur. In fact, when the truncation error is included, equation (5) resembles the viscous transonic equation, which has been

used to simulate shock structure (Hayes, 1958). The difference equations exhibit similar behaviour, automatically locating shock waves in the form of compression bands spread over a few mesh widths.

The calculations to be described are based on a similar principle, but use a coordinate invariant difference scheme in which the retarded difference formulas are constructed to conform with the local flow direction. The resulting 'rotated' difference scheme allows complete flexibility in the choice of a coordinate system. Thus curvilinear coordinates may be used without restriction to improve the accuracy of the treatment of boundary conditions, and mesh points can be concentrated in regions of rapid variation of the flow. The property of automatically locating shock waves is retained. This is a great advantage in treating flows which may contain a complex pattern of waves. The scheme has proved to be stable and convergent throughout the transonic range, including the case of flight at Mach 1. Calculations have been performed for Mach numbers up to 1.2 and yaw angles up to 60° , covering the most likely operating range of a yawed wing transport designed to fly at slightly supersonic speeds. The calculations become progressively less accurate, however, towards the upper end of the range, because the difference scheme is first order accurate in the supersonic zone. Also the present scheme has the disadvantage that it is not written in conservative form (Lax, 1954), so that the correct jump conditions are not precisely enforced. The best way to improve the treatment of the jump conditions remains an open question.

2. Formulation in Curvilinear Coordinates.

The configuration to be considered is illustrated in Figure 1. An isolated wing is placed at an arbitrary yaw angle in a uniform free stream with prescribed Mach number at infinity. According to the Kutta condition the viscous effects cause the circulation at each span station to be such that the flow passes smoothly off the sharp trailing edge. The varying spanwise distribution of lift generates a vortex sheet which trails in the streamwise direction behind the trailing edge, and behind the side edge of the downstream tip. In practice the vortex sheet rolls up behind each tip and decays through viscous effects. A simplified model will be used in which convection and decay of the sheet are ignored. Then the jump Γ in potential should be constant along lines parallel to the free stream behind the wing. Also the normal component of velocity should be continuous through the sheet. At infinity the flow is undisturbed except in the Trefftz plane far downstream, where there will be a two dimensional flow induced by the vortex sheet.

Near the leading edge the boundary surface has a high curvature. In order to prevent a loss of accuracy in the numerical treatment of the boundary condition it is convenient to use curvilinear coordinates. Then by making the body coincide with a coordinate surface, we can avoid the need for complicated interpolation formulas, and maintain small truncation errors. For two dimensional calculations an effective way to do this is to map the exterior of the profile onto a regular shape, such as a circle or half plane, by a conformal mapping (Sells, 1968; Garabedian and Korn, 1972; Jameson 1974). For three dimensional calculations no such simple method is available. The number of additional terms in the equations arising from coordinate transformations should be limited to avoid an excessive growth in the computer time required for a calculation. For this reason the use of a conformal transformation which varies in the spanwise direction is not attractive.

A convenient coordinate system for treating wings with straight leading edges can be constructed in two stages. Let x , y and z be Cartesian coordinates with the x - y planes containing the wing sections, and the z axis parallel to the leading edge, as in Figure 1. Then the wing is first 'unwrapped' by a square root transformation of the x - y planes, independent of z ,

$$x + iy = \frac{1}{2} (X_1 + iY_1)^2, \quad z = Z_1 \quad (6)$$

applied about a singular line just behind the leading edge, as in Figure 2. X_1 and Y_1 represent parabolic coordinates in the x - y planes, which become half planes in X_1 and Y_1 , while the wing surface is split open to form a bump on the boundary $Y_1 = 0$. In terms of the transformed coordinates the surface can be represented as

$$Y_1 = S(X_1, Z_1) \quad (7)$$

In the second stage of the construction the bump is removed by a shearing transformation in which the coordinate surfaces are displaced until they become parallel to the wing surface:

$$X = X_1, \quad Y = Y - S(X_1, Z_1), \quad Z = Z_1 \quad (8)$$

The final coordinates X , Y and Z are slightly nonorthogonal. It is best to continue the sheared coordinate surfaces in the direction of the mean camber line off the trailing edge, so that there is no corner in the coordinate lines if the wing has a cusped trailing edge. The vortex sheet is assumed to lie in the surface $Z = 0$ so that it is also split by the transformation. A complication is caused by the continuation of the cut beyond the wing tips. Points on the two sides

of the cut map to the same point in the Cartesian system, and must be identified when writing difference formulas. While the leading edge is restricted to be straight, the wing section can be varied or twisted and the trailing edge can be tapered or curved in any desired manner. The yaw angle is introduced simply by rotating the flow at infinity. It is then necessary to track the edge of the vortex sheet in the streamwise direction.

Since the potential approaches infinity in the far field, it is necessary to work with a reduced potential G , from which the singularity at infinity has been removed. If θ is the yaw angle, and α the angle of attack in the crossplane normal to the leading edge, we set

$$\phi = G + \left\{ \frac{1}{2}[X^2 - (Y+S)^2] \cos \alpha + X(Y+S) \sin \alpha \right\} \cos \theta + Z \sin \theta \quad (9)$$

Orthogonal velocity components in the X_1, Y_1 and Z_1 directions are then

$$\begin{aligned} U &= \frac{1}{h} \left\{ G_X - S_X G_Y + [X \cos \alpha + (Y+S) \sin \alpha] \cos \theta \right\} \\ V &= \frac{1}{h} \left\{ G_Y + [X \sin \alpha - (Y+S) \cos \alpha] \cos \theta \right\} \\ W &= G_Z - S_Z G_Y + \sin \theta \end{aligned} \quad (10)$$

where h is the mapping modulus of the parabolic transformation given by

$$h^2 = X^2 + (Y+S)^2 \quad (11)$$

The local speed of sound now satisfies the relation

$$a^2 = a_0^2 - \frac{\gamma-1}{2} (U^2 + V^2 + W^2) \quad (12)$$

The potential equation becomes

$$AG_{XX} + BG_{YY} + CG_{ZZ} + DG_{XY} + EG_{YZ} + FG_{XZ} = H \quad (13a)$$

where

$$\begin{aligned} A &= a^2 - U^2 \\ B &= a^2(1 + S_X^2 + h^2 S_Z^2) - (V - US_X - h^2 WS_Z)^2 \\ C &= h^2(a^2 - W^2) \\ D &= -2a^2 S_X - 2U(V - US_X - h^2 WS_Z) \\ E &= -h^2 a^2 S_Z - 2h(V - US_X - h^2 WS_Z)W \\ F &= -2hUW \end{aligned} \quad (13b)$$

and

$$\begin{aligned} H &= \left\{ (a^2 - U^2) S_{XX} + h^2 (a^2 - W^2) S_{ZZ} - 2hUWS_{XZ} \right\} G_Y \\ &+ \left\{ (U^2 - V^2) \cos \alpha + 2UV \sin \alpha \right\} \cos \theta \\ &- \frac{1}{h} (U^2 + V^2) \left\{ UX + V(Y+S) \right\}. \end{aligned} \quad (13c)$$

The boundary condition on the body takes the form

$$G_Y = - \frac{(S \cos \alpha - X \sin \alpha) \cos \theta + U_1 S_X + h^2 W_1 S_Z}{1 + S_X^2 + h^2 S_Z^2} \quad (14a)$$

where

$$\begin{aligned} U_1 &= G_X + (X \cos \alpha + S \sin \alpha) \cos \theta \\ W_1 &= G_Z + \sin \theta \end{aligned} \quad (14b)$$

An advantage of the parabolic transformation is that it collapses the height of the disturbance due to the vortex sheet to zero in the transformed coordinate system at points far downstream, where X approaches infinity. Thus the far field boundary condition is simply

$$G = 0 \quad (15)$$

In order to obtain a finite region for computation the coordinates X , Y and Z may finally be replaced by stretched coordinates. For example one can set

$$X = \frac{\bar{X}}{(1 - \bar{X}^2)^\alpha}$$

where α is a positive index, so that \bar{X} varies between -1 and 1 as X varies between $-\infty$ and ∞ .

3. Numerical Scheme.

The success of the Murman difference scheme for the small disturbance equation (5) is attributable to the fact that the use of retarded difference formulas in the supersonic zone leads to the correct region of dependence, and also introduces a truncation error which acts like viscosity. The artificial viscosity is added smoothly because the coefficient of ϕ_{xx} is zero at the sonic line, where the switch in the difference scheme takes place.

The 'rotated' difference scheme employed for the present calculations is designed to introduce correctly oriented upwind difference formulas in a similar smooth manner when the flow direction is arbitrary. With this end in view, the equation is rearranged as if it were locally expressed in a coordinate system aligned with the flow. Considering first the case of Cartesian coordinates, let s denote the stream direction. Then equation (1) can be written in the canonical form

$$(a^2 - q^2) \phi_{ss} + a^2 (\Delta \phi - \phi_{ss}) = 0 \quad (16)$$

where q is the stream speed determined from the formula

$$q^2 = u^2 + v^2 + w^2 \quad (17)$$

and $\Delta\phi$ denotes the Laplacian

$$\Delta\phi = \phi_{xx} + \phi_{yy} + \phi_{zz} \quad (18)$$

Since the direction cosines of the stream direction are u/q , v/q , and w/q , the streamwise second derivative can be expressed as

$$\phi_{ss} = \frac{1}{q^2} (u^2\phi_{xx} + v^2\phi_{yy} + w^2\phi_{zz} + 2uv\phi_{xy} + 2vw\phi_{yz} + 2uw\phi_{xz}) \quad (19)$$

On substituting the expressions for ϕ_{ss} and $\Delta\phi$, equation (16) reduces to the usual form (1). To carry out this rearrangement ϕ_x , ϕ_y and ϕ_z are first evaluated using central difference formulas. With the velocity components known, the local type of the flow is determined from the sign of $a^2 - q^2$. If the flow is locally subsonic all terms are represented by central difference formulas. If, on the other hand, it is locally supersonic, all second derivatives contributing to ϕ_{ss} in the first term are represented by retarded difference formulas of the form

$$\phi_{xx} = \frac{\phi_{i,j,k} - 2\phi_{i-1,j,k} + \phi_{i-2,j,k}}{\Delta x^2}$$

$$\phi_{xy} = \frac{\phi_{i,j,k} - \phi_{i-1,j,k} - \phi_{i,j-1,k} + \phi_{i-1,j-1,k}}{\Delta x \Delta y}$$

biased in the upstream direction in each coordinate, while the remaining terms are represented by central difference formulas. The scheme assumes a form similar to the Murman scheme whenever the velocity coincides with one of the coordinate directions. At subsonic points it is second order accurate. At supersonic points it is first order accurate, introducing an artificial viscosity proportional to $q^2 - a^2$ which just vanishes at the sonic line,

When the equation is written in curvilinear coordinates, only the principal part, consisting of the terms containing the second derivatives on the left-hand side of equation (13a), need be split and rearranged in this way, since the characteristic directions and region of dependence are determined by the coefficients of the second derivatives. Also the expressions for the second derivatives dominate the finite difference equations when the mesh width is small. Accordingly all terms contributing to H on the right side of (13a) are calculated using central difference formulas at both supersonic and subsonic points.

It remains to devise a scheme for solving the difference equations. The presence of downstream points in the central difference

formulas prevents the use of a simple marching procedure in either the supersonic or the subsonic zone. Thus we are led to use an iterative method. At each cycle the difference formulas are evaluated using old values of the potential, generated during the previous cycle, at points which have not yet been updated. While iterative methods are well established for elliptic equations, the use of such a method in the supersonic zone, where the equation is hyperbolic, requires analysis. For this purpose it is convenient to regard the iterations as steps in an artificial time coordinate, so that the solution procedure can be considered as a finite difference scheme for a time dependent equation. Provided that the iterative process is stable and consistent with a properly posed initial value problem, the time dependent equation will represent its behaviour in the limit as the mesh is refined. Thus we can infer the behaviour of the iterative process from the behaviour of the equivalent time dependent equation. If the process is to converge, the solution of the steady state equation ought to be a stable equilibrium point of the time dependent equation, and the regions of dependence of the two equations should be compatible.

Denoting updated values by a superscript +, representative central difference formulas for the second derivatives are

$$G_{XX} = \frac{G_{i-1,j,k}^+ - (1+r\Delta X)G_{i,j,k}^+ - (1-r\Delta X)G_{i,j,k} + G_{i+1,j,k}}{\Delta X^2} \quad (20)$$

$$G_{XY} = \frac{G_{i+1,j+1,k} - G_{i-1,j+1,k} - G_{i+1,j-1,k} + G_{i-1,j-1,k}}{4\Delta X\Delta Y}$$

where old values of the potential are used on one side because the new values are not yet available, and a linear combination of old and new values is used at the center point. If Δt is the time step these formulas may be interpreted as representing

$$G_{XX} - \frac{\Delta t}{\Delta x} (G_{Xt} + rG_t)$$

and

$$G_{XY} - \frac{1}{2} \frac{\Delta t}{\Delta x} G_{Yt}$$

Thus the presence of mixed space time derivatives cannot be avoided in the equivalent time dependent equation. This equation can therefore be written in the form

$$(M^2 - 1)G_{SS} - G_{mm} - G_{nn} + 2\alpha_1 G_{st} + 2\alpha_2 G_{mt} + 2\alpha_3 G_{nt} = Q \quad (21)$$

where M is the local Mach number,

$$M = \frac{Q}{a} \quad (22)$$

m and n are suitably scaled coordinates in the plane normal to the stream direction s , and Q contains all terms except the principal part. The coefficients α_1 , α_2 , and α_3 depend on the split between new and old values in the difference equations. Introducing a new time coordinate

$$T = t - \frac{\alpha_1 s}{M^2 - 1} + \alpha_2 m + \alpha_3 n \quad (23)$$

equation (21) becomes

$$(M^2 - 1)G_{SS} - G_{mm} - G_{nn} - \left(\frac{\alpha_1^2}{M^2 - 1} - \alpha_2^2 - \alpha_3^2 \right) G_{TT} = Q. \quad (24)$$

To avoid producing an ultrahyperbolic equation for which the initial data cannot in general be arbitrarily prescribed (Courant and Hilbert, 1962), the difference formulas at supersonic points should be organized so that

$$\alpha_1^2 > (M^2 - 1)(\alpha_2^2 + \alpha_3^2). \quad (25)$$

Then the hyperbolic character is retained by the time dependent equation, and s is the time like direction as in the steady state equation.

If condition (25) is satisfied, the characteristic cone of the time dependent equation (21) is given by

$$(\alpha_2 s - \alpha_1 m)^2 + (\alpha_3 s - \alpha_1 n)^2 - (M^2 - 1)(\alpha_3 m - \alpha_2 n)^2 + (M^2 - 1)(t^2 + 2\alpha_2 m t + 2\alpha_3 n t) - 2\alpha_1 s t = 0$$

This is illustrated in Figure 3 for the two dimensional case. The region of dependence lies entirely behind the current time level except for the single characteristic direction

$$t = 0, \quad m = \frac{\alpha_2}{\alpha_1} s, \quad n = \frac{\alpha_3}{\alpha_1} s.$$

The difference equations will have the correct region of dependence provided that the points are ordered so that the backward half of this line lies in the updated region. The mechanism of convergence in the supersonic zone can also be inferred from the orientation of the characteristic cone. Since the region of dependence lies entirely on the upstream side, with advancing time it will eventually cease to intersect the initial time plane. Instead it will intersect a surface containing the Cauchy data of the steady state problem, and hence the solution will reach a steady state. The rate of convergence is maximized by minimizing the rearward inclination of the most retarded characteristic

$$t = \frac{2\alpha_1}{M^2-1} s, \quad m = -\frac{\alpha_2}{\alpha_1} s, \quad n = -\frac{\alpha_3}{\alpha_1} s.$$

Thus it is best to use the minimum value of α_1 which allows condition (25) to be satisfied.

Condition (25) generally requires the retarded difference formulas for G_{SS} in the supersonic zone to be augmented by expressions contributing to the term in G_{st} . At the same time a local von Neumann test (Jameson, 1974) indicates that at supersonic points the new and old values ought to be split so that the coefficient of ϕ_t in the equivalent time dependent equation is zero. For these reasons, and also to ensure the diagonal dominance of the equations for the new values on each line, G_{SS} is calculated at supersonic points using formulas of the form

$$G_{XX} = \frac{2G_{i,j,k}^+ - G_{i,j,k} - 2G_{i-1,j,k}^+ + G_{i-2,j,k}}{\Delta X^2}$$

$$G_{XY} = \frac{G_{i,j,k}^+ - G_{i-1,j,k}^+ - G_{i,j-1,k}^+ + G_{i-1,j-1,k}^+}{\Delta X \Delta Y} \quad (26)$$

where the superscript + has again been used to denote new values. The first formula can be interpreted as representing

$$G_{XX} + 2 \frac{\Delta t}{\Delta x} G_{Xt}.$$

Its use together with the corresponding formulas for G_{YY} and G_{ZZ} thus results in the introduction of a term in G_{st} proportional to the coefficient $q^2 - a^2$ of G_{SS} . To meet condition (25) near the sonic line, where $q^2 - a^2$ approaches zero, the coefficient of ϕ_{st} can be further augmented by adding a term

$$\beta \frac{\Delta t}{\Delta x} (UG_{Xt} + VG_{Yt} + h^2 WG_{Zt}) \quad (27)$$

with β an appropriately chosen positive parameter. The required mixed space time derivatives are represented by formulas of the form

$$\frac{\Delta t}{\Delta x} G_{Xt} = \frac{G_{i,j,k}^+ - G_{i,j,k} - G_{i-1,j,k}^+ + G_{i-1,j,k}}{\Delta X^2} \quad (28)$$

The treatment of the principal part at supersonic points is completed by using central difference formulas of the form (20) to represent $\Delta\phi - \phi_{SS}$, with r set equal to zero to give a zero coefficient of ϕ_t .

In the subsonic zone formulas of the form (20) are used for all second derivatives. Convergence now depends on the damping provided

by ϕ_t (Garabedian, 1956). If ω is the overrelaxation factor one takes

$$r \Delta x = \frac{2}{\omega} - 1 \quad (29)$$

where ω has a value slightly less than 2. In both the subsonic and the supersonic zones the velocities and all terms containing the first derivatives are evaluated by formulas of the form

$$G_X = \frac{G_{i+1,j,k} - G_{i-1,j,k}}{2\Delta X}$$

using values frozen from the previous cycle.

The boundary condition at the body is satisfied by giving appropriate values to G at a row of dummy points behind the boundary. The standard difference equations are then used at the surface points, which are thus treated with similar truncation errors to the interior points. To treat lifting flows it is necessary to allow for a jump Γ in the potential between corresponding points in the plane $Y = 0$, representing the two sides of the vortex sheet. The jump should be constant along lines in the streamline direction. Difference formulas bridging the cut are evaluated using a value of Γ frozen from the previous cycle. At the end of the cycle Γ is then adjusted to the new value of the jump at the appropriate point on the trailing edge.

The foregoing formulas represent a point relaxation algorithm. To increase the speed of convergence it is better to use a line relaxation algorithm in which all the points on a line are simultaneously updated. If points on an X line are being updated, the only modification required is to replace the central difference formula (20) for G_{XX} by a formula using all new values

$$G_{XX} = \frac{G_{i-1,j,k}^+ - 2G_{i,j,k}^+ + G_{i+1,j,k}^+}{\Delta X^2}$$

The resulting line equations are easily solved, since they are tri-diagonal and diagonally dominant in both the subsonic and the supersonic zones. The lines to be updated can be in any coordinate direction. The only constraint is the need to march in a direction which is not opposed to the flow, in order to obtain a positive coefficient for G_{st} . It has been found best to divide each X - Y plane into three strips. Then one marches towards the surface in the central strip, and outwards with the flow in the left and right-hand strips.

4. Results.

FORTTRAN computer programs incorporating these principles have been used to make extensive numerical studies of both two and three dimensional transonic flows. To save computer time, calculations are performed on a sequence of meshes. The solution is first obtained on a coarse mesh. This is then interpolated to provide the starting point for a calculation in which the mesh size is halved in each coordinate direction. Using this procedure the lift can be approximately determined on the coarse mesh at very low cost. Typically the lattice for the initial calculation contains 64 divisions in the chord-wise X direction, 8 divisions in the normal Y direction, and 16 divisions in the spanwise Z direction, giving 8,192 cells. The refined mesh then has 65,536 cells. Generally 200 cycles on the coarse mesh followed by 100 cycles on the fine mesh are sufficient to reduce the largest residual to the order of 10^{-5} . Such a calculation takes about 30 minutes on a CDC 6600. To improve the resolution of the shocks on the wing surface, more divisions are sometimes used in the X coordinate, giving a refined mesh with $192 \times 16 \times 32 = 98,304$ cells. In order to check the convergence of the method as the mesh size is reduced, a few calculations have been made on a sequence of three meshes, with $192 \times 32 \times 64 = 393,216$ cells on the third mesh. Such a calculation requires the use of the disc for storage, and is expensive. Each fine mesh cycle takes about 90 seconds, so that a complete calculation takes 3 or 4 hours. For engineering purposes the meshes with 65,536 or 98,304 cells generally seem to give sufficient accuracy.

A useful test of the accuracy of the three-dimensional difference scheme is provided by the case of an infinite yawed wing. The conditions for simple sweepback theory are then exactly satisfied, and the flow is effectively two-dimensional. If the yaw angle is varied to keep the velocity normal to the leading edge fixed as the Mach number is increased, the only change should be in the uniform spanwise component of the velocity. The flow in the planes containing the wing section should be independent of the yaw angle. It is treated differently by the difference scheme, however, because the size of the hyperbolic region increases as the Mach number and yaw angle are increased, so that retarded differencing is used at a larger number of points. Figure 4 shows a comparison of the computed pressure distribution over an infinite yawed wing at two corresponding conditions, Mach .65 with zero yaw, and Mach 1.02 with a yaw angle of 50.4° . The wing section was designed by Garabedian to produce very high lift

with shockfree flow (Bauer, Garabedian, Jameson and Korn, 1974), and the flow is very sensitive to small changes in the Mach number and angle of attack. The lift and drag coefficients obtained by integrating the surface pressure are also shown. For convenience all coefficients are referred to the velocity normal to the leading edge. It can be seen that the numerical results do have the expected invariance despite the change in the differencing. These calculations were performed with a mesh containing 240 divisions in the X coordinate and 32 divisions in the Y coordinate.

Figures 5, 6 and 7 show typical results of calculations for finite wings. The pressure distributions at successive span stations are plotted above each other at equal vertical intervals, with the leading tip at the bottom. In all cases the computed lift drag ratio includes an allowance for a skin friction coefficient of .010. At positive yaw angles the contribution of the spanwise force component has been ignored to avoid errors arising from poor resolution at the tips. Figures 5 and 6 display results of calculations using the very fine mesh with 393,216 cells. Figure 5 shows an example at Mach .75 with zero yaw. The wing section is one used by R.T. Jones in tests of a model with yawed wing (Graham, Jones and Boltz, 1973). Two-dimensional calculations show that this section generates two shock waves at low lift which coalesce to a single shock wave at high lift. It is interesting that the three dimensional flow shows a transition from the single to the double shock pattern as the load falls off near the tips. Figure 6 shows an example for a wing with the same section at Mach .866 and a yaw angle of 30° . The angle of attack is the angle measured in the plane normal to the leading edge. Some twist was introduced, but not enough to equalize the load completely. At this yaw angle the shock waves are still quite well captured by the difference scheme, as can be seen. Figure 7 shows an example of a calculation on a mesh with 98,304 cells. The wing section was another airfoil designed by Garabedian. In two dimensional flow this airfoil should be shock free at a Mach number of .80 and a lift coefficient of .3, with supersonic zones on both upper and lower surfaces. The wing is shown at Mach .87 and a yaw angle of 15° . Shock waves can be clearly seen on both surfaces. The calculations indicate, however, that with this moderate amount of sweep, and some relief due to the three dimensional effects, drag rise is only just beginning to occur at this point. Since this airfoil is also 12 percent thick, it is an attractive candidate for a fast subsonic airplane such as an executive jet.

With a supersonic free stream and a large yaw angle, the flow is generally supersonic behind the oblique shock waves which appear on the wing surface. In this situation the computed shock waves are less well defined. Usually they are spread over 4 or 5 mesh widths. The calculations still appear, however, to provide a useful estimate of the lift drag ratio. Figure 8 shows some curves of the lift drag ratio for a partially tapered wing with Jones' section and an aspect ratio of 11.1. These were computed using a mesh with 65,536 cells. The amount of twist was generally not correctly chosen to equalize the load across the span. The curves are, however, quite consistent with the results of Jones' tests of a yawed wing with the same section and an elliptic planform of aspect ratio 12.7.

5. Conclusion

The results support the belief that with the speed and capacity of the computers now in prospect it will be possible to use the computer as a 'numerical wind tunnel'. The use of an artificial time dependent equation results in rapid convergence, in contrast to methods in which the physical time dependent equation is integrated until it reaches a steady state (Magnus and Yoshihara, 1970). The consistency of the results also provides a numerical confirmation of the uniqueness of weak solutions of the potential equation, provided that the correct entropy inequality is enforced.

Much remains to be done to improve the accuracy and range of the calculations. In order to improve the treatment of the shock waves it would be better to write the equations in conservative form. This requires only a small modification of the small disturbance equation (5). The first term is expressed in the form $\frac{\partial r}{\partial x}$ where

$$r = (1-M_\infty^2)\phi + \frac{\gamma+1}{2}\phi_x^2$$

Artificial viscosity should then be introduced in a conservative form. This can be done by subtracting the term

$$P_{i,j,k} - P_{i-1,j,k}$$

where

$$P_{i,j,k} = \begin{cases} 0 & , \text{ at subsonic points} \\ \frac{r_{i+1,j,k} - r_{i-1,j,k}}{2\Delta x} & , \text{ at supersonic points} \end{cases}$$

This results in an artificial viscosity proportional to $\partial^2 r / \partial x^2$ in the supersonic zone. At the sonic line it is equivalent to the use of Murman's new shock point operator (Murman, 1973).

The appropriate conservation law for the full potential equation expresses conservation of mass

$$\frac{\partial}{\partial x} (\rho u) + \frac{\partial}{\partial y} (\rho v) + \frac{\partial}{\partial z} (\rho w) = 0$$

where the density ρ is given by the formula

$$\rho = \{1 + \frac{\gamma-1}{2} M^2 (1-u^2-v^2-w^2)\}^{1/(\gamma-1)} .$$

The analogue of the Murman scheme introduces a truncation error proportional to $(\partial^2 / \partial x^2) (\rho u)$ in the supersonic zone by retarded differencing. Numerical tests of such a scheme have shown it to be less accurate than the simple retarded scheme for the potential equation, because of the additional errors arising from this term. Shock waves standing above the surface in a two dimensional flow must be normal because the flow turns smoothly. Thus they can be located at points of transition to subsonic flow. An approximation to the jump conditions could then be directly imposed. This approach is less promising for three dimensional calculations, because it is not so simple to locate the shock waves.

Another shortcoming of the present scheme is its use of first order accurate difference equations at supersonic points. Consequently, if the supersonic zone is large, a very fine mesh is needed to obtain an accurate answer. One line of investigation is the addition of an explicit term in ϕ_{tt} to the artificial time dependent equation. This would rotate the characteristic cone back from the current time level, allowing more latitude for the construction of a higher order scheme. The resulting second order equation can also be reduced to a first order system of equations in a form amenable to standard differencing procedures.

The treatment of more complicated configurations such as wing-body combinations will require extensive investigations of the best way to set up a coordinate system. It may prove most economical to patch together separate regions, each using its own coordinate system suited to the local flow pattern.

Acknowledgement

This work has been supported by the U. S. Atomic Energy Commission under Contract No. AT(11-1)-3077 with New York University and by NASA under Grant No. 33-016-167. It has greatly benefited from the advice and suggestions of Paul Garabedian. The author is also indebted to Frances Bauer for important help in carrying out some of the computer runs.

Bibliography

1. Bailey, F. R., and Ballhouse, W. F., Relaxation methods for transonic flows about wing-cylinder combinations and lifting swept wings, Third Int. Congress on Numerical Methods in Fluid Dynamics, Paris, July 1972.
2. Bauer, F., Garabedian, P., and Korn, D., Supercritical wing sections, Springer-Verlag, New York, 1972.
3. Bauer, F., Garabedian, P., Jameson, A., and Korn, D., Handbook of supercritical wing sections, to be published as a NASA special publication, 1974.
4. Courant, R., and Hilbert, D., Methods of Mathematical Physics, Vol. 2, Interscience-Wiley, New York, p. 758 (1962).
5. Garabedian, P. R., Estimation of the relaxation factor for small mesh size, Math. Tables Aids Comp., 10, 183-185 (1956).
6. Garabedian, P., and Korn, D., Analysis of transonic airfoils, Comm. Pure Appl. Math., 24, 841-851 (1972).
7. Graham, Lawrence A., Jones, Robert T., and Boltz, Frederick W., An experimental investigation of three oblique-wing and body combinations at Mach numbers between .60 and 1.40. NASA TM X-62, 256 (1973).
8. Hayes, Wallace D., The basic theory of gas dynamic discontinuities, Section D, Fundamentals of Gas Dynamics, edited by Howard W. Emmons, Princeton (1958).
9. Jameson, Antony, Transonic flow calculations for airfoils and bodies of revolution, Grumman Aerodynamics Report 390-71-1, December 1971.
10. Jameson, Antony, Iterative solution of transonic flows over airfoils and wings including flows at Mach 1, to appear in Comm. Pure Appl. Math. (1974).
11. Jones, R. T., Reduction of wave drag by antisymmetric arrangement of wings and bodies, AIAA Journal, 10, 171-176 (1972).

12. Lax, Peter D., Weak solutions of nonlinear hyperbolic equations and their numerical computation, *Comm. Pure Appl. Math.*, 7, 159-193 (1954).
13. Magnus, R., and Yoshihara, H., Inviscid transonic flow over airfoils, *AIAA Jour.* 8, 2157-2162 (1970).
14. Morawetz, C. S., On the nonexistence of continuous transonic flows past profiles, *Comm. Pure Appl. Math.* 9, 45-68 (1956)
15. Murman, E. M., and Cole, J. D., Calculation of plane steady transonic flows, *AIAA Jour.* 9, 114-121 (1971)
16. Murman, Earl M., Analysis of embedded shock waves calculated by relaxation methods, *AIAA Conf. on Computational Fluid Dynamics*, Palm Springs, July 1973.
17. Sells, C. C. L., Plane subcritical flow past a lifting airfoil, *Proc. Roy. Soc. London*, 308A, 377-401 (1968).
18. Steger, J. L., and Lomax, H., Transonic flow about two dimensional airfoils by relaxation procedures, *AIAA Jour.* 10, 49-54 (1972).

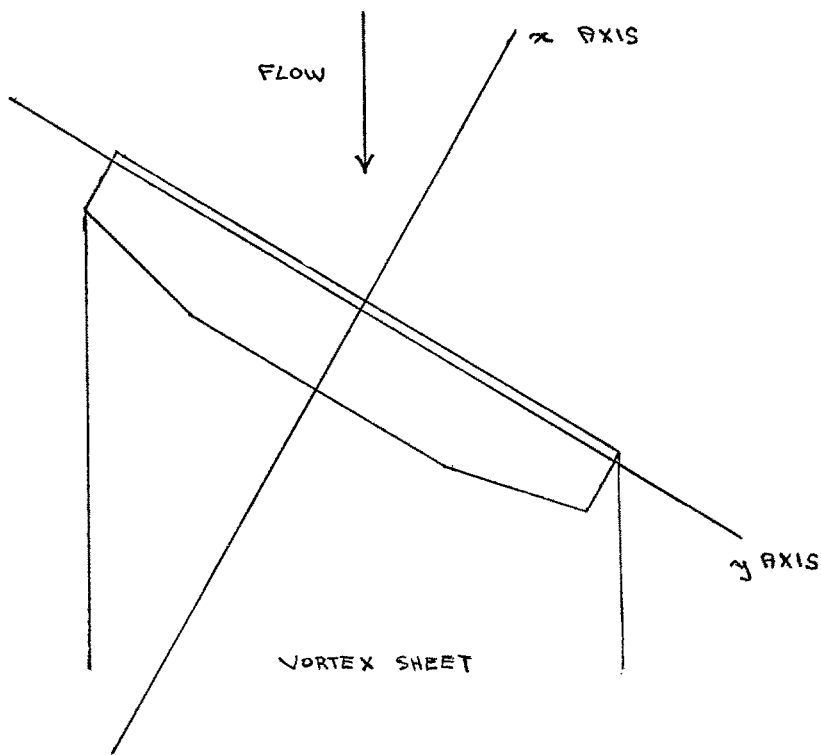


Figure 1
CONFIGURATION

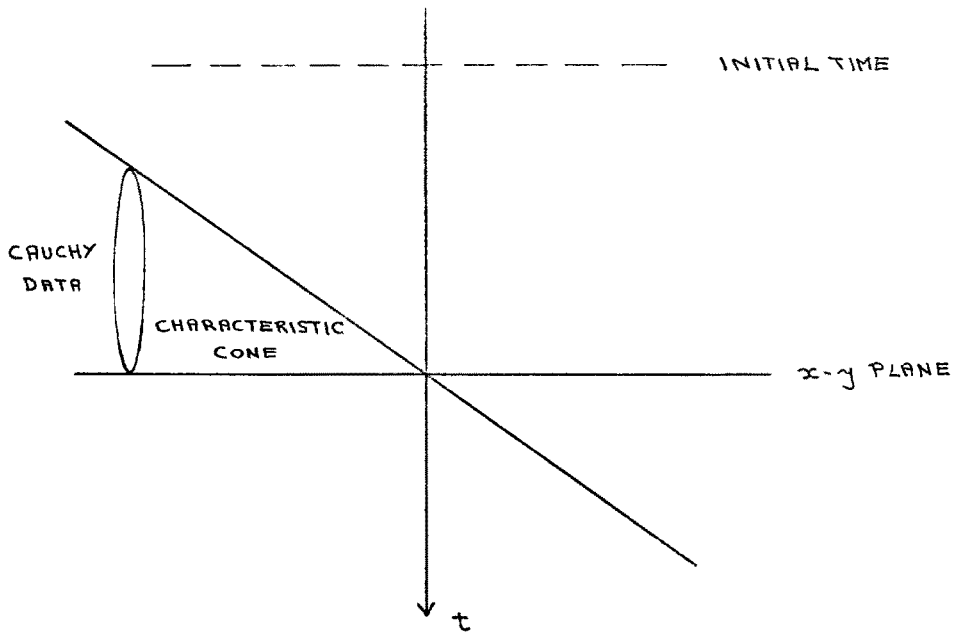
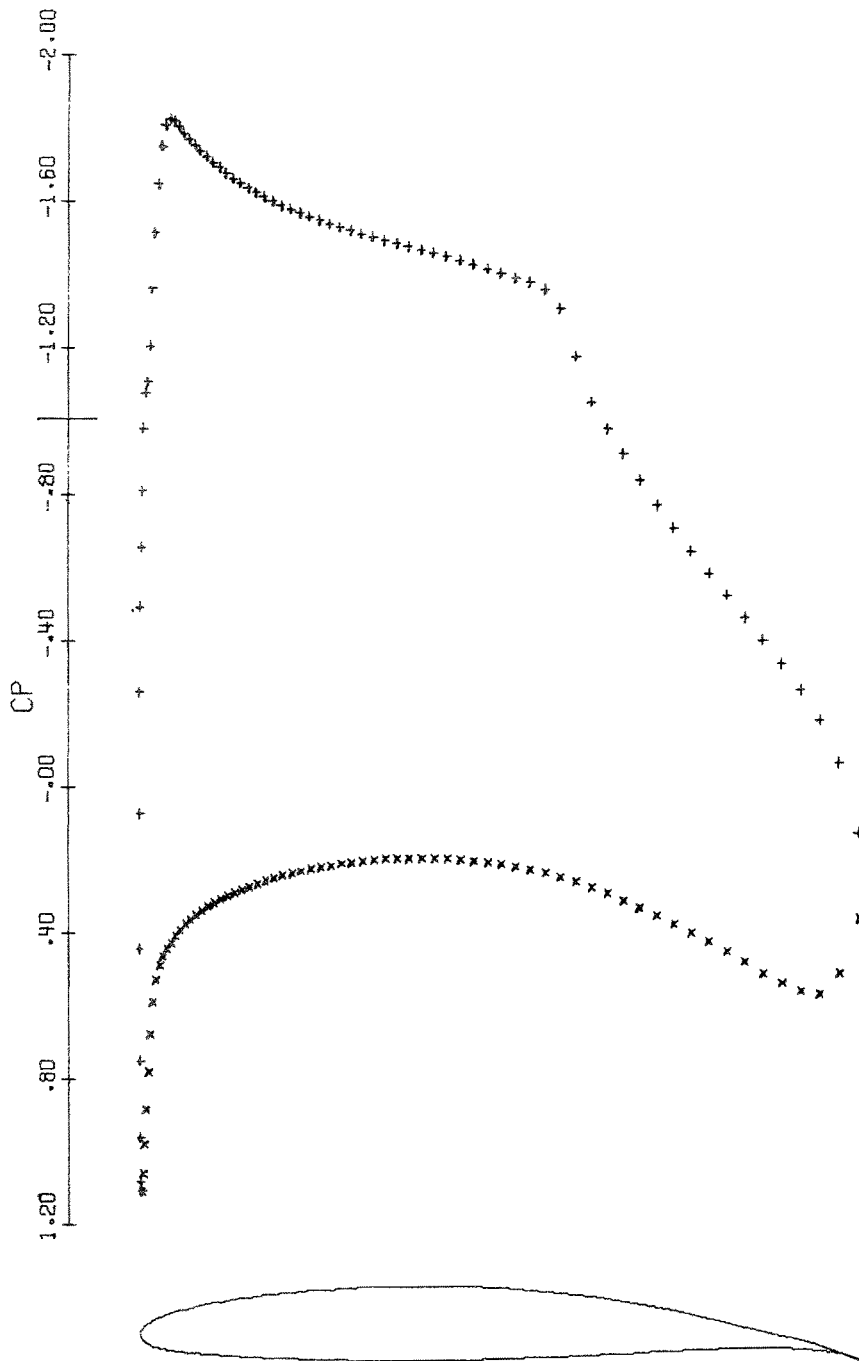


FIGURE 3

CHARACTERISTIC CONE OF EQUIVALENT TIME DEPENDENT EQUATION
FOR TWO DIMENSIONAL FLOW

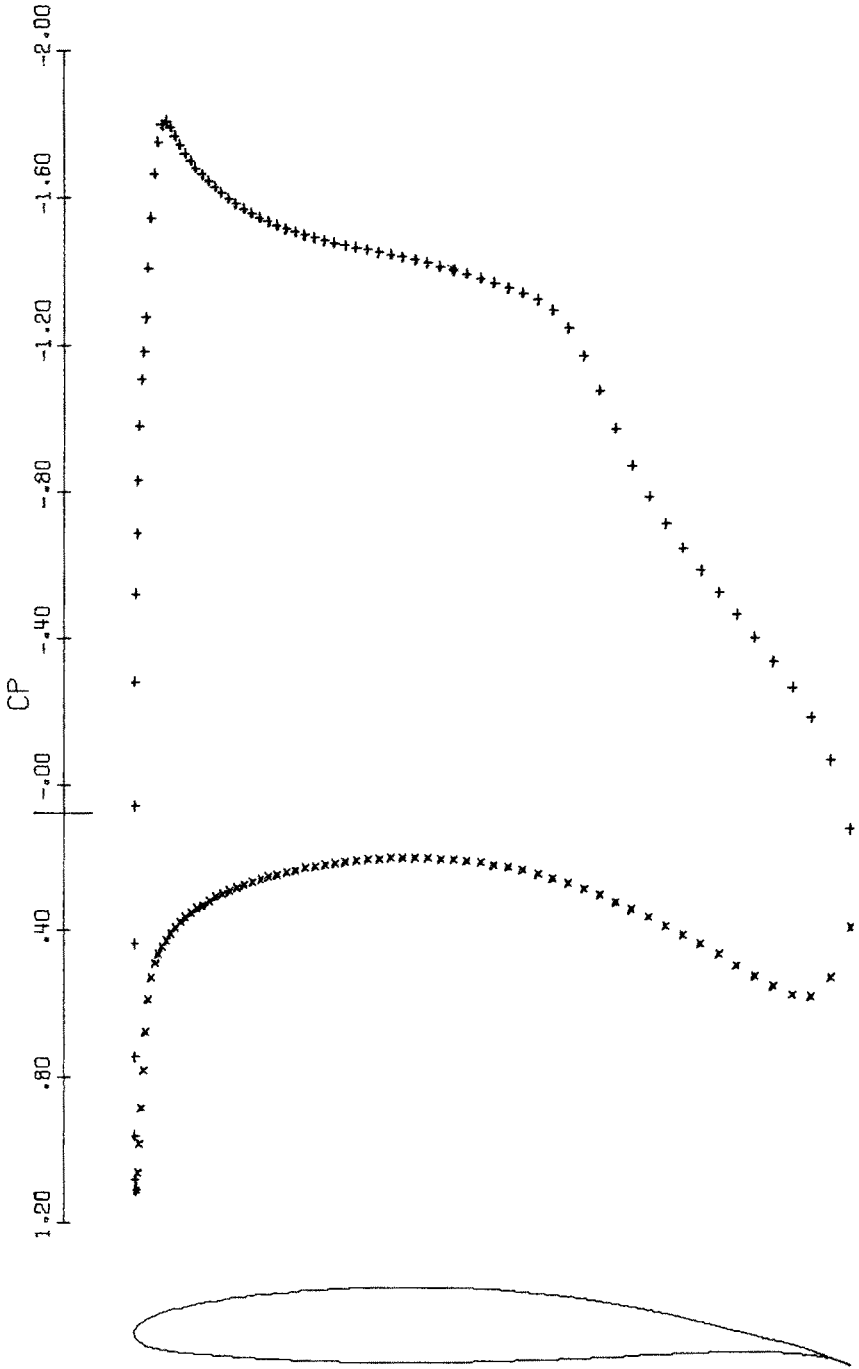


G 65-15 AIRFOIL

M = .650 YAW = 0.000 ALF = -0.000

CL = 1.4661 CD = .0001

Figure 4(a)



G 65-15 AIRFOIL

M = 1.020 YAW = 50.410 ALF = -0.000

CL = 1.4575 CD = .0032

Figure 4(b)

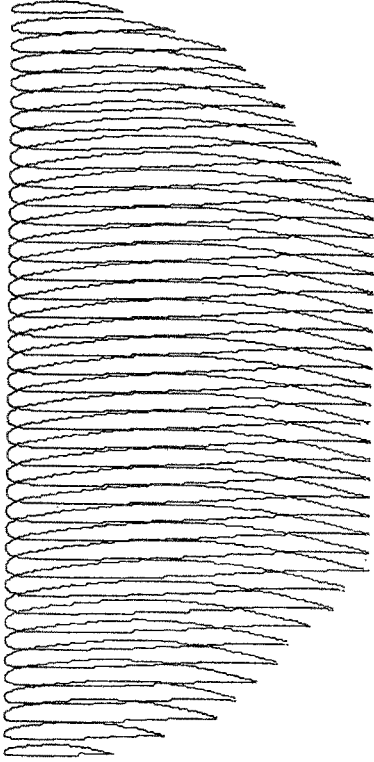


Figure 5(a). View of Wing

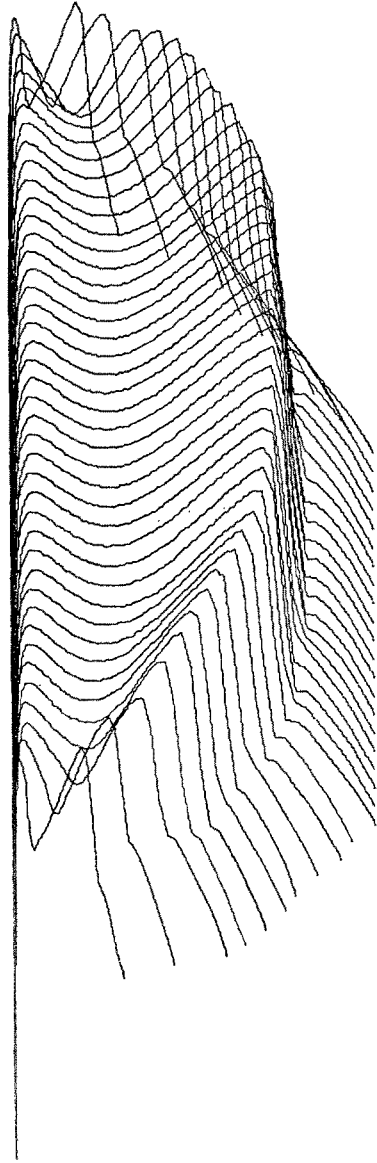


Figure 5(b). Upper Surface Pressure

JONES SECTION	AR 11.6	TWIST 0 DEG
M = .750	YAW = 0.00	ALF = 3.00
L/D = 18.02	CL = 1.0414	CD = .0578

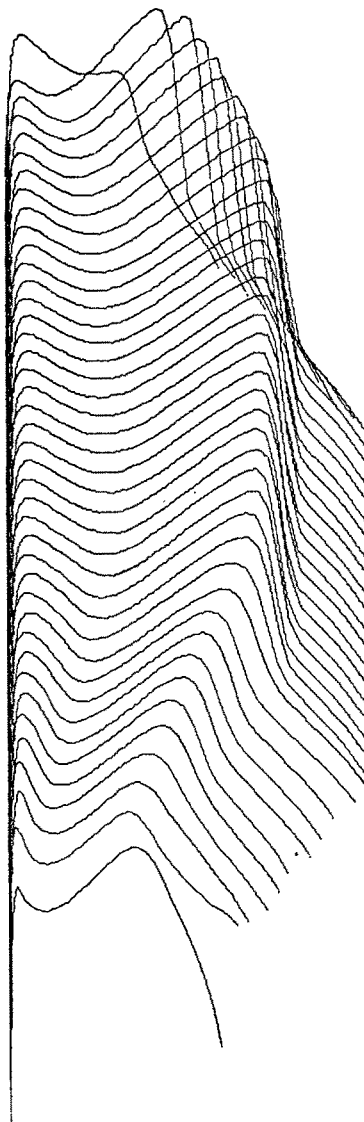
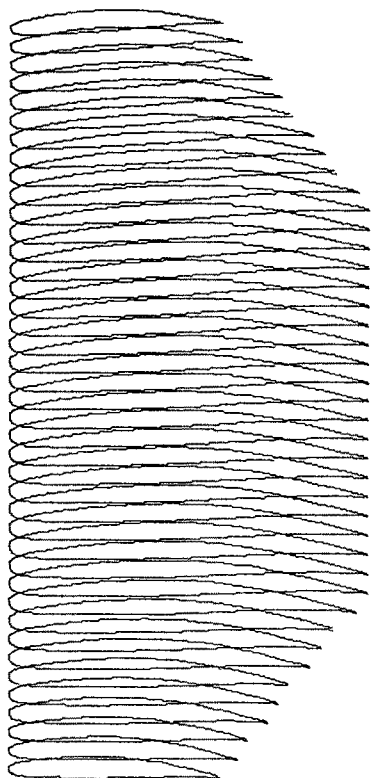


Figure 6(a). View of Wing.

Figure 6(b). Upper Surface Pressure

JONES SECTION AR 13.3 TWIST 4 DEG
M = .866 YAW = 30.00 ALF = 3.00
L/D = 16.71 CL = .7474 CD = .0447

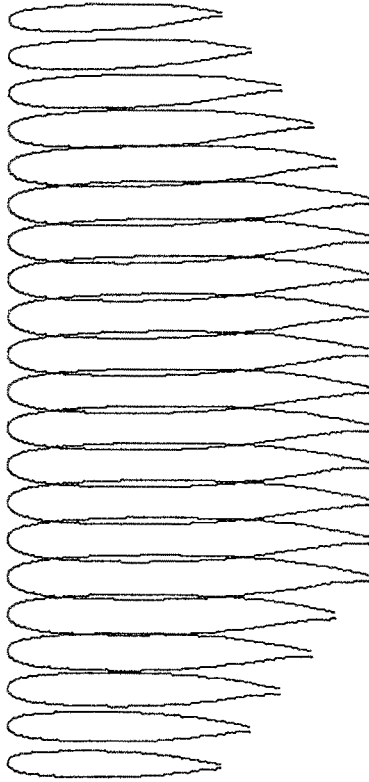


Figure 7(a)

VIEW OF WING
G 80-30 SECTION AR 6.6 TWIST 3 DEG
M = .870 YAW = 15.00 ALF = .90
L/D = 14.90 CL = .2566 CD = .0172

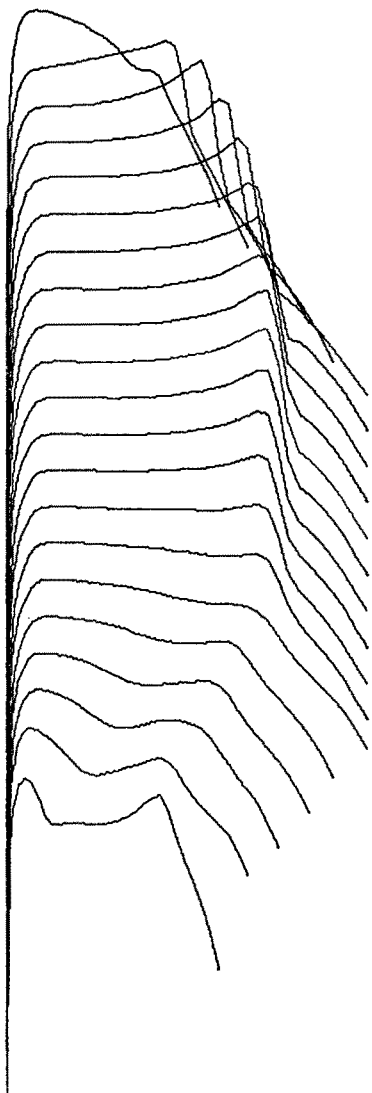


Figure 7(b). Upper Surface Pressure.

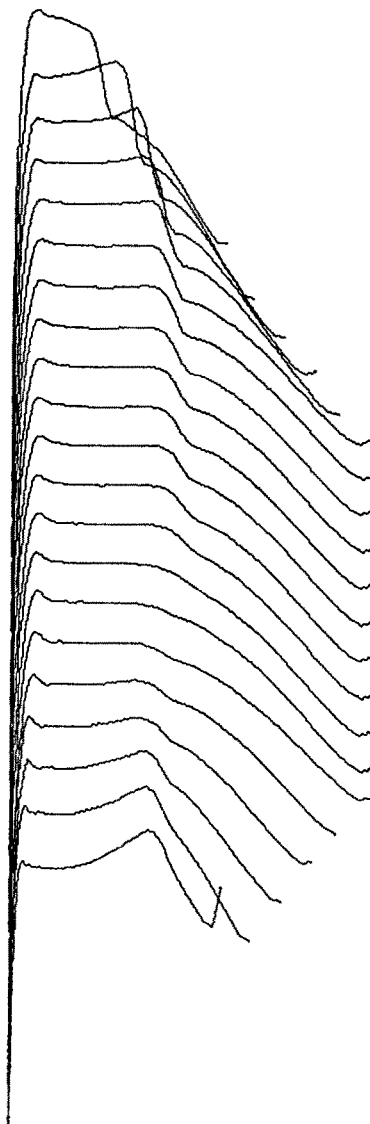


Figure 7(c). Lower Surface Pressure.

G 80-30 SECTION	AR	6.6	TWIST	3 DEG
M = .870	YAW =	15.00	ALF =	.90
L/D = 14.90	CL =	.2566	CD =	.0172

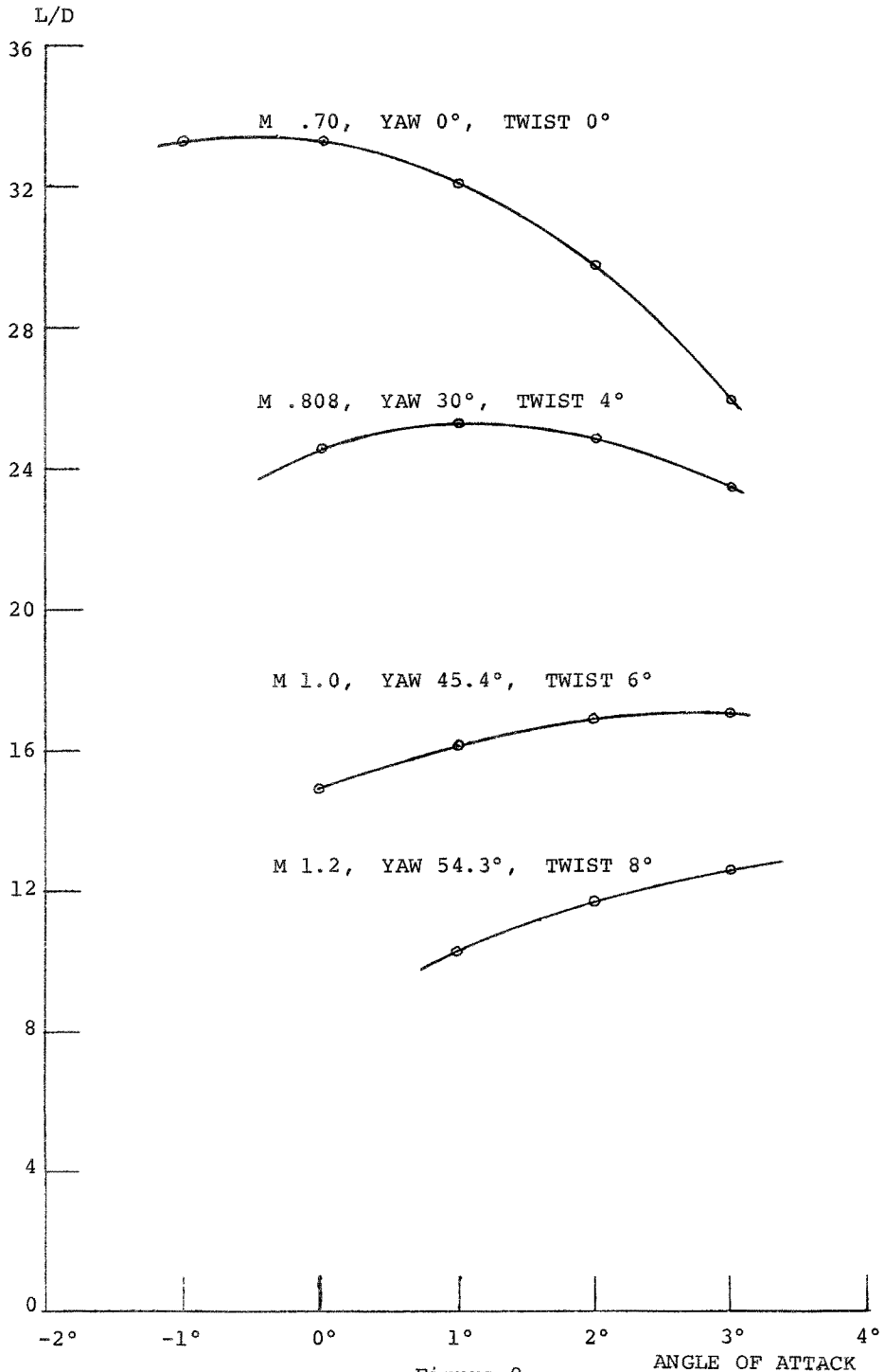


Figure 8
LIFT DRAG RATIO FOR A YAWED WING OF ASPECT RATIO 11.1
WITH JONES' SECTION.